

Article

Study on Vertical Load-Carrying Capacity of Post-Grouting Bored Piles

Dezhi Kong *, Heng Li  and Wensong Gan

School of Civil Engineering and Architecture, Henan University, Kaifeng 475004, China;
liheng_xiangwan@126.com (H.L.); wensonggan77@126.com (W.G.)

* Correspondence: 10160005@vip.henu.edu.cn

Abstract: The relationship between pile side frictional resistance and pile tip resistance and settlement is assumed to be ideal elastic–plastic. The load-transfer method is used to analyze the load-bearing characteristics of bored pile in actual projects, and the results are compared with static load test results to prove the reliability of the analysis method and its parameters, on the basis of which the bored piles are reinforced with grouting, namely, pile tip grouting, pile side grouting, and pile tip–pile side composite grouting, are analyzed. The results show that the pile tip grouting mainly improves pile tip resistance and has almost no effect on pile side frictional resistance; the pile side grouting improves pile tip resistance and pile side frictional resistance more significantly; and pile tip–pile side composite grouting improves pile tip resistance and pile side frictional resistance more significantly than the first two. The ultimate load-carrying capacity of the pile is increased by 19%, 49%, and 53% after the use of pile tip grouting, pile side grouting, and composite grouting respectively.

Keywords: load transfer; grouting; bored pile



Citation: Kong, D.; Li, H.; Gan, W. Study on Vertical Load-Carrying Capacity of Post-Grouting Bored Piles. *Appl. Sci.* **2022**, *12*, 7452. <https://doi.org/10.3390/app12157452>

Academic Editor: Daniel Dias

Received: 11 June 2022

Accepted: 22 July 2022

Published: 25 July 2022

Publisher's Note: MDPI stays neutral with regard to jurisdictional claims in published maps and institutional affiliations.



Copyright: © 2022 by the authors. Licensee MDPI, Basel, Switzerland. This article is an open access article distributed under the terms and conditions of the Creative Commons Attribution (CC BY) license (<https://creativecommons.org/licenses/by/4.0/>).

1. Introduction

At present, pile foundation is the main form of foundation in engineering construction. Bored pile is one of the more widely used pile types, and its vertical bearing capacity is mainly from pile side frictional resistance and pile tip resistance. However, due to the influence of stratigraphic conditions and piling technique, bored pile inevitably produces pile side mud skin and pile tip sediment, so the vertical bearing capacity of the pile foundation cannot be fully developed [1,2].

According to the literature [3], post-grouting reinforcement technology was first used in 1958 by Venezuela in the construction of the Maracaibo bridge using grouting tube to reinforce the pile in the bridge foundations, and was tested and found to have significantly improved the pile-bearing capacity. Bu et al. [4] conducted static load tests on bored pile and post-grouting bored pile in a trial piling project for the Sutong Yangtze River Bridge. The results showed that the ultimate bearing capacity of the pile after grouting increased by 1.48 to 2.0 times and the total pile tip resistance increased by 2.46 to 7.21 times. It is believed that the slurry increases the strength of the soil at the pile tip and part of the soil around the pile by permeating and compacting the soil layer, thus increasing the ultimate bearing capacity of the pile. Zhai et al. [5] carried out static load tests on three piles of a supertall project and investigated the load-bearing characteristics of large-diameter, extralong bored pile using numerical analysis. The ultimate load-carrying capacity of pile with pile tip grouting was found to increase by almost 50% compared to ungrouted pile, and the ultimate load-carrying capacity of piles with composite pile tip–pile side grouting was found to roughly double. Wan et al. [6] established a method for calculating the bearing capacity of post-grouting pile applicable to different grouting types by analyzing a large number of post-grouting static load test data.

Many other scholars have also summarized many ultimate bearing-capacity calculation formulae for post-grouting pile in their research, mainly based on the calculation

formulae for the bearing capacity of ordinary pile with the introduction of corresponding enhancement factors for consideration according to the different grouting methods [7]. This method is an empirical formula based on actual measurements under specific conditions, and its applicability is somewhat limited by various conditions in the project, such as the difference of grouting amount. This paper analyzes the load-transfer law of bored pile in conjunction with actual engineering and the effect on the load transfer of pile after the use of reinforcement methods, such as pile tip grouting, pile side grouting, and composite grouting. In the engineering design stage, the difference in geological conditions and the amount of grouting provides the corresponding theoretical basis for the prediction of the ultimate pile-bearing capacity.

2. Pile Load-Transfer Analysis

The pile is generally elastic in its work. According to the theory of elasticity, the pile displacement w under vertical load is related to the pile side frictional resistance q_s as follows

$$B \frac{\partial^2 w}{\partial z^2} = Uq_s \tag{1}$$

where B is the pile compressive stiffness and U is the perimeter of pile section.

Since in practical engineering, pile generally traverses multiple layers of soil, the solution for the pile side frictional resistance needs to consider the influence of the nature of different soil layers on the pile side frictional resistance in addition to the factor of pile displacement. Seed et al. [8] proposed the load-transfer method to express the relationship between pile lateral resistance and pile displacement as

$$q_s = q_s(w) \tag{2}$$

This relationship is known as the load-transfer function and can be solved for using the pile balance condition and deformation coordination conditions.

Due to the different properties and transfer functions of the soil layers on the side of the pile, the specific calculations are analyzed by dividing the pile into several segments (as in Figure 1a). For segment i pile unit (as in Figure 1b) the top surface settlement is w_{i-1} and the bottom surface settlement is w_i .

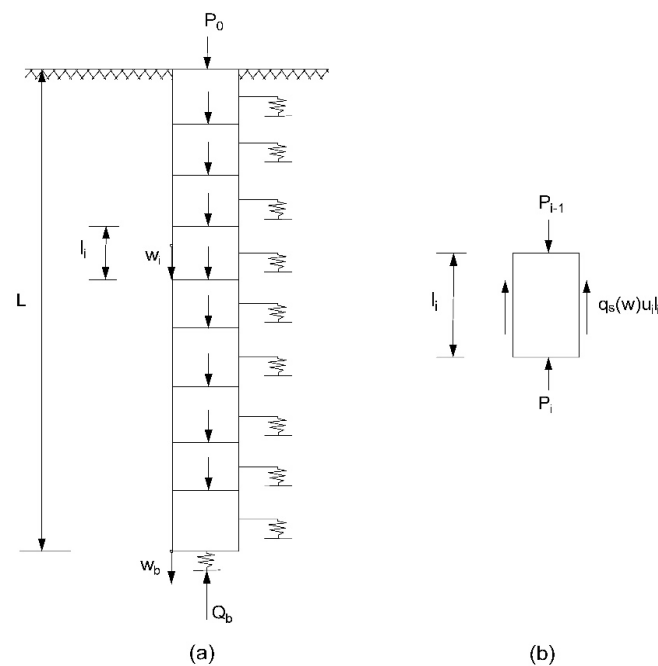


Figure 1. Pile-soil interaction model:(a) Pile force diagram; (b) Pile unit force diagram.

Based on the load-transfer function, the side frictional resistance q_{si} can be obtained for the segment i pile unit, and the total side frictional resistance for the segment i pile unit can be approximated as

$$Q_{si} = q_{si}u_i l_i \quad (3)$$

where u_i is the perimeter of the section of the segment i pile unit and l_i is the length of the segment i pile unit.

Let the top surface axial force and bottom surface axial force of the segment i pile unit be P_{i-1} , P_i , respectively, then according to the balance condition of the pile body, we get

$$Q_{si} = P_{i-1} - P_i \quad (4)$$

Approximate the average axial force of the segment i pile unit as

$$N_i = \frac{P_{i-1} + P_i}{2} \quad (5)$$

Considering the pile body as an elastomer, the compression of the segment i pile unit is

$$\Delta_i = \frac{N_i}{E_{ci}A_{ci}}l_i \quad (6)$$

where E_{ci} is the elastic modulus of the segment i bored pile and A_{ci} is the cross-sectional area of the segment i bored pile.

According to the deformation compatibility condition, then

$$\Delta_i = w_{i-1} - w_i \quad (7)$$

Using the pile balance and deformation compatibility conditions, the pile axial force, the pile side frictional resistance, and the pile settlement at the unit division interface of each pile segment can be calculated.

For multilayer soils, the specific calculation uses the iterative method, presupposing a smaller pile tip settlement w_b . Based on the load-transfer function, the relationship between the pile tip resistance q_p and the pile tip settlement w_b is

$$q_p = q_p(w_b) \quad (8)$$

The pile tip resistance q_p is calculated from Equation (8), and assuming a uniform distribution of pile tip resistance, the total pile tip resistance Q_b is

$$Q_b = q_p A_b \quad (9)$$

where A_b is the pile tip cross-sectional area.

According to the balance condition and deformation compatibility condition of the pile body, the bottom settlement w_n and bottom axial force P_n of the segment n pile unit are

$$bw_n = w_b \quad (10)$$

$$P_n = Q_b \quad (11)$$

The values of the top surface settlement w_{n-1} and top surface axial force P_{n-1} of the segment n pile unit, which satisfy both the pile balance condition and the deformation compatibility condition, are then calculated by iteration. Similarly, calculating from the bottom up can get the top surface settlement w_{n-2} , w_{n-3} , \dots , w_0 of each pile unit and the top axial force P_{n-2} , P_{n-3} , \dots , P_0 of each pile unit. Afterwards, the presupposition settlement at the pile tip is increased appropriately, the value w_b is reset, and the calculation is again iterated from the segment n pile unit upwards to obtain the top surface settlement of each pile unit and the top axial force of each pile unit under the new pile tip settlement.

Increase the value of w_b until both the pile side and the soil at the pile tip have fully yielded, at which point P_0 is the ultimate bearing capacity of the pile. The relationship between pile top load and pile top displacement and the distribution of pile axial force and pile side frictional resistance force along the depth can be obtained from the calculation results.

3. Engineering Example

3.1. Engineering Overview

A residential building project in Kaifeng has 18 floors above ground and 2 floors below ground (including underground garage), with a total floor area of 11,167.1 m² above ground and a frame shear wall structure as the main body. The stratigraphic conditions were measured by Henan Province Non-ferrous Engineering Survey Limited after on-site drilling and sampling and soil tests, such as physical property test, direct shear test, and consolidation test, the results of which are shown in Table 1.

Table 1. Stratigraphic conditions.

Soil Layer Number	Soil Layer	Layer Thickness (m)	Unit Weight (kN/m ³)	Water Content (%)	Cohesion (kPa)	Internal Friction Angle (°)	Compression Modulus $E_{s1,2}$ (MPa)
(1)	Silt	2.9	18.7	23.3	12	22.7	9.6
(2)	Silt with silty clay	5.3	18.9	26.4	13	22.7	6.3
(3)	Silt	3.4	19.1	25.5	10	23.7	9.6
(4)	Silt with silty clay	2.6	18.8	26.9	12	19.2	7.0
(5)	Silt with silty sand	7.2	19.2	25.4	11	25.5	13.2
(6)	Silty clay	0.8	19.2	23.1	21	23.4	8.6
(7)	Fine sand	12.0	20.6	—	0	30.5	22.0

The foundation is designed as a pile raft foundation, with a depth of 6.2 m for the bearing platform and reinforced concrete bored pile for the foundation. The pile concrete cube compressive strength is 30 MPa, pile diameter $d = 500$ mm, pile length $L = 20$ m. According to the design specification, the ultimate vertical bearing capacity of a single pile is 1800 kN and the standard bearing capacity 900 kN. The project set up a total of 192 bored piles.

3.2. Pile Calculation Analysis

For the calculation and analysis of this bored pile using the load-transfer method, the load-transfer function Equations (2) and (8) should be determined first. Since Seed proposed the load-transfer method, many scholars have also proposed many transfer function models on this basis [9–12], and these models have laid the foundation for load-transfer analysis of pile. The calculations in this paper use the Kezdi ideal elastic–plastic model with the load-transfer functions of the pile tip on the pile side as follows, respectively

$$q_s = \begin{cases} k_s w, w < w_u \\ k_s w_u, w \geq w_u \end{cases} \quad (12)$$

$$q_p = \begin{cases} k_b w_b, w_b < w_{bu} \\ k_b w_{bu}, w_b \geq w_{bu} \end{cases} \quad (13)$$

where k_s is the stiffness factor of the side frictional resistance of the pile segment, w_u is the critical value of pile settlement when the soil in which the pile segment is located reaches yield, k_b is the stiffness factor of the soil resistance at the pile tip, and w_{bu} is the critical value of pile tip settlement when the soil at the pile tip reaches yield.

The static load test was carried out 28 days after the completion of the pile construction by Kaifeng City Yellow River Engineering Quality Inspection Limited by means of platform surcharge load. The test was carried out by means of a pile foundation static load tester (model RS-JYB) for loading, a displacement transducer (model RSWS-50) to measure the settlement of the single pile under step-by-step loading, and a pressure transducer (model

ST3000LBCIIE7RY) that was placed at the jack to measure the pile top load. According to the values of pile axial force shaft and pile settlement measured in the static load test of this project, the relationship between pile side frictional resistance and pile settlement in (2) soil layer is shown in Figure 2.

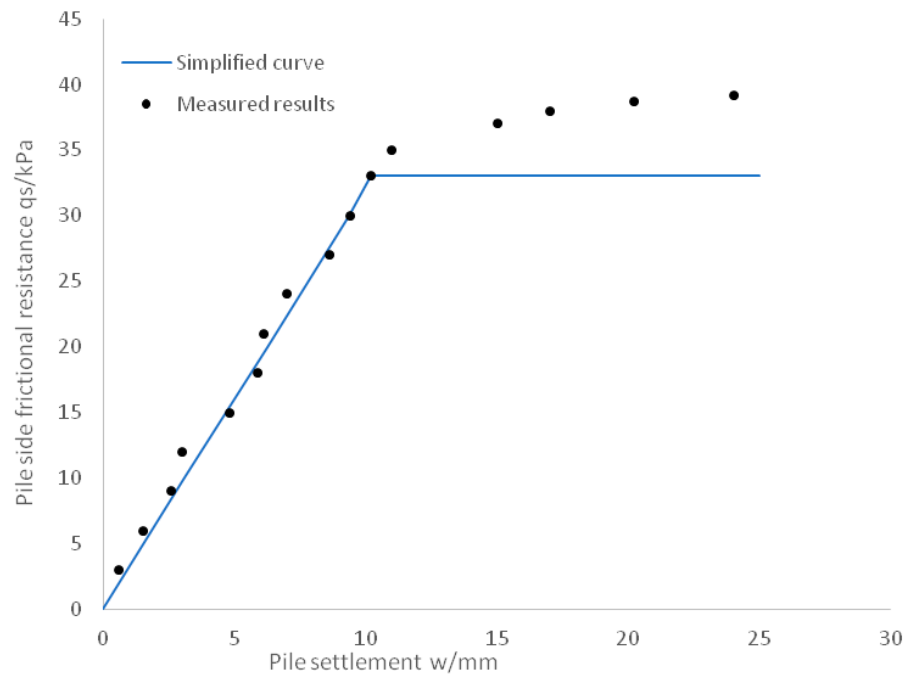


Figure 2. Measured results and simplified curve of pile lateral resistance vs. pile settlement for soil layer (2).

From Figure 2, it can be seen that the ultimate pile side frictional resistance of soil layer (2) is 33 kPa and the corresponding ultimate pile settlement is 10.2 mm. Model parameters for other soil layers are obtained similarly and the results are shown in Table 2.

Table 2. Load-transfer model parameters.

Soil Layer Number	Soil Layer	q_s (kPa)	q_p (kPa)	w_u (mm)	w_{bu} (mm)	k_s (kPa/mm)	k_b (kPa/mm)
(2)	Silt with silty clay	33		10.2		3.2	
(3)	Silt	47		9.5		4.9	
(4)	Silt with silty clay	38		10.6		3.9	
(5)	Silt with silty sand	52		9.2		5.7	
(6)	Silty clay	48		10.8		4.4	
(7)	Fine sand	64	1500	10.0	11.5	6.4	130.4

The pile was divided into 18 segments for the calculation, and the length of each segment and the soil layer in which it is located are shown in Table 3.

Table 3. Length of each pile segment and the soil layer in which it is located.

Pile Segment Number	1–2	3–5	6–7	8–13	14	15–18
Segment length(m)	1.00	1.13	1.30	1.20	0.80	1.00
Soil layer number	(2)	(3)	(4)	(5)	(6)	(7)

The pile tip settlements w_b are preset to be 1.0 mm, 3.0 mm, 5.0 mm, 7.0 mm, 9.0 mm, 11.0 mm, 11.5 mm, and 12.0 mm respectively. Calculations based on the iterative method

described in Section 1 of this paper. The pile top settlement w_0 and the pile top load P_0 under each pile tip settlement w_b are shown in Table 4.

Table 4. Calculation of pile top settlement w_0 and pile top load P_0 under each pile tip settlement w_b .

w_b (mm)	1.0	3.0	5.0	7.0	9.0	11.0	11.5	12.0
w_0 (mm)	1.4	4.2	7.0	9.8	12.5	14.8	15.3	15.8
P_0 (kN)	208	623	1038	1453	1747	1841	1854	1854

The relationship between pile top load and pile top settlement was plotted according to Table 4 and compared with the Kaifeng City Yellow River Engineering Quality Inspection Limited results of static load tests at the engineering site, as shown in Figure 3.

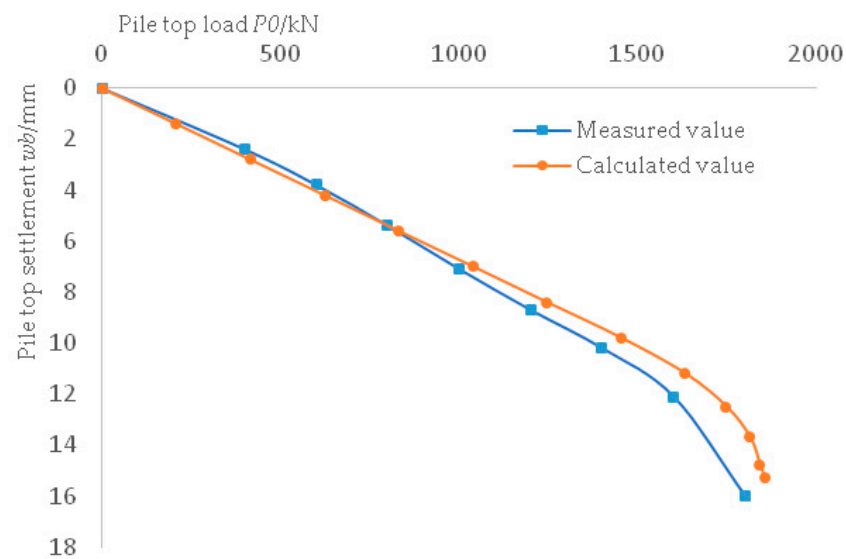


Figure 3. Relationship between pile top load P_0 and pile top settlement w_0 .

As can be seen from Figure 3, the calculated pile top load settlement relationship curves and the pile top load settlement relationship curves from the static load test are basically the same, and both show a steep drop. The ultimate load capacity of the bored pile obtained from the static load test is 1800 kN and the corresponding settlement at the top of the pile is 16 mm, while the ultimate load at the top of the bored pile is 1854 kN and the corresponding settlement at the top of the pile is 15.3 mm, which are close to each other and prove that the parameters chosen for this calculation are reasonable.

4. Effect of Grouting on the Performance of Bored Pile

In order to study the effect of grouting reinforcement on the load-bearing performance of piles, three types of grouting methods, namely, pile tip grouting, pile side grouting, and pile tip–pile side composite grouting, were analyzed.

4.1. Calculation Model for Post-Grouting Bored Pile

As the cement slurry under pressure will have a permeating, compacting [13], and fracturing [14] effect on the soil around the pile, the soil on the side of the pile and the soil at the tip of the pile were reinforced to form a cement soil consolidation body around the pile and at the pile tip. During injection, the slurry is cemented within the diffusion range through each grouting hole, forming an approximate columnar reinforcement with the soil around the pile (as shown in Figure 4). Therefore, the cement soil consolidation body in the grouting segment combined with the original pile can be regarded as a composite pile segment of equal cross-section in the calculation.

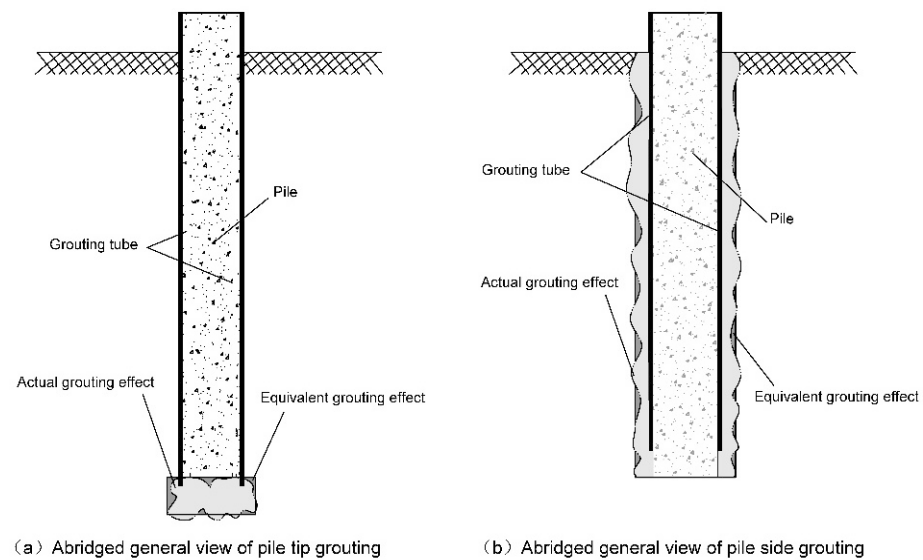


Figure 4. Pile tip and pile side grouting abridged general view of bored pile.

The compression of the pile in the grouting segment is:

$$\Delta_i = \frac{N_i}{E_{ci}A_{ci} + E_{pi}A_{pi}} l_i \quad (14)$$

$$A_p = \frac{\pi}{4} [(d + 2R)^2 - d^2] \quad (15)$$

where E_{pi} is the elastic modulus of the segment i of the cement soil consolidation body, A_{pi} is the cross-sectional area of the segment i of the cement soil consolidation body, and R is the diffusion radius after grouting.

According to the diffusion theory of Magg [15], the diffusion radius R after grouting is

$$R = \sqrt[3]{\frac{3kh_0r_0t}{\beta n}} \quad (16)$$

where k is the soil permeability coefficient, h_0 is the grouting pressure head, r_0 is the grouting tube radius, t is the grouting time, β is the ratio of slurry viscosity to water viscosity, and n is the porosity of the soil

Considering that in the actual grouting, if the diffusion radius is small, the enhancement effect on the pile is not obvious, if the diffusion radius is large, it is difficult to implement in the project, so this paper selects the diffusion radius R as 100 mm. Pre-embedding of 20 mm diameter grouting steel tube on the pile circumference surface was considered. The ratio of slurry viscosity to water viscosity β is 0.95. The soil permeability coefficient k and the porosity of the soil n are selected according to Equation (16) for different soil layers and the corresponding grouting pressure head h_0 and grouting time t are selected according to the diffusion radius R . As there are multiple layers of soil in the actual project and the properties of different soils vary, the amount of cement injected into the soil needs to be used to roughly predict the soil conditions in which the slurry will be located in order to adjust the grouting pressure and grouting time accordingly. After reinforcement by grouting, the grouting pile segment can be treated as a composite pile segment with a pile diameter of 700 mm.

In order to ensure the effect of grouting, the cement soil consolidation body should have a certain strength, selected consolidation body strength of 5 MPa, and the corresponding mixing ratio 25% was obtained by taking soil samples from each layer of the site and conducting ratio tests in the laboratory. The cement soil test specimens were made according to the mixing ratios obtained from the tests and were subjected to compression

tests. The modulus E_{50} of the cement soil was measured to be 295–372 MPa. The calculation takes the modulus E_p of the cement soil consolidation body as 300 MPa.

4.2. Calculation of Vertical Ultimate Load under Pile Tip Grouting Conditions

In order to analyze the effect of different grouting thickness at the pile tip on the performance of the pile, grouting thicknesses of 0.2 m, 0.5 m, 0.7 m, and 1.0 m were selected for the calculations. The pile segment is calculated as before, with the cement soil consolidation body at the tip of the pile as the 19th pile segment unit, and the load transfer parameters between the composite pile and the soil after grouting are still taken (Tables 1 and 2). Calculations were carried out based on the iterative method described in Section 1, and the load settlement relationships for the pile at different grouting thickness obtained from the results are shown in Figure 5.

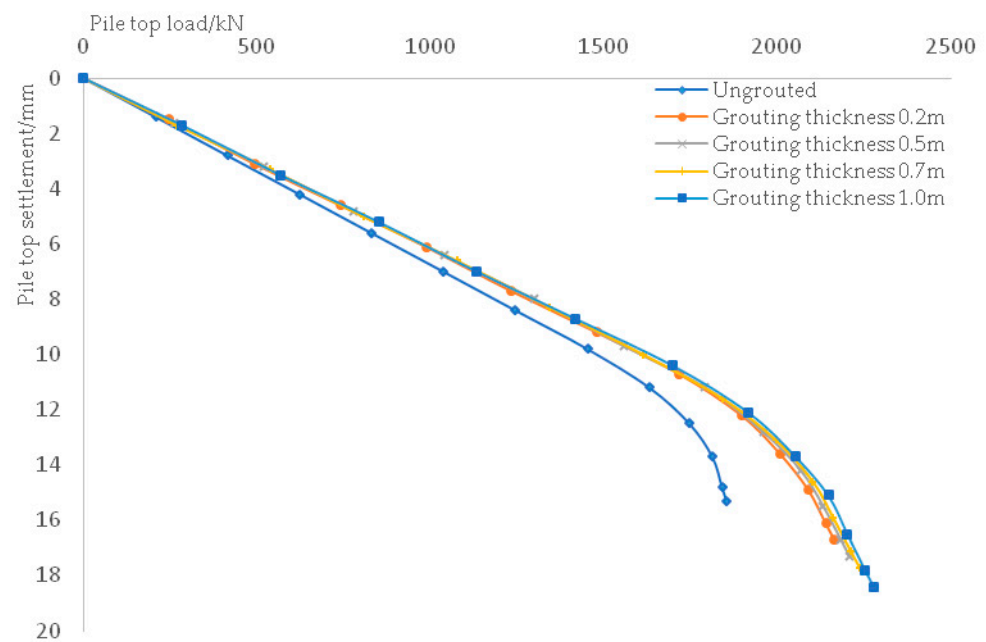


Figure 5. Load settlement relationship for pile with different grouting thickness.

It can be seen from Figure 5 that the ultimate load capacity of the pile is increased after the pile tip grouting and the settlement at the top of the pile also increases, and increases with the increase of the grouting thickness.

The ultimate pile top load and the corresponding values of the total pile side frictional resistance and total pile tip resistance for different grouting thickness are calculated, and the relationship between the three and the pile tip grouting thickness is shown in Figure 6.

As can be seen from Figure 6, the increase in pile load capacity is mainly due to the increase in pile tip resistance, while the increase in pile side frictional resistance is very limited. This is due to the fact that the slurry spreads under pressure into the soil layer at the tip of the pile, creating an enlarged head that increases the cross-sectional area at the bottom of the pile with very limited increase in the side area of the pile. The pile tip resistance is thus increased and the pile side frictional resistance is only slightly increased, while with the increase in grouting thickness the cross-sectional area at the bottom of the pile no longer increases and the total pile side area continues to increase, so the pile tip resistance no longer increases and the pile side frictional resistance increases, but only to a very limited extent. From the results, it appears that the pile tip grouting mainly improves the pile tip resistance and has less effect on the pile side resistance.

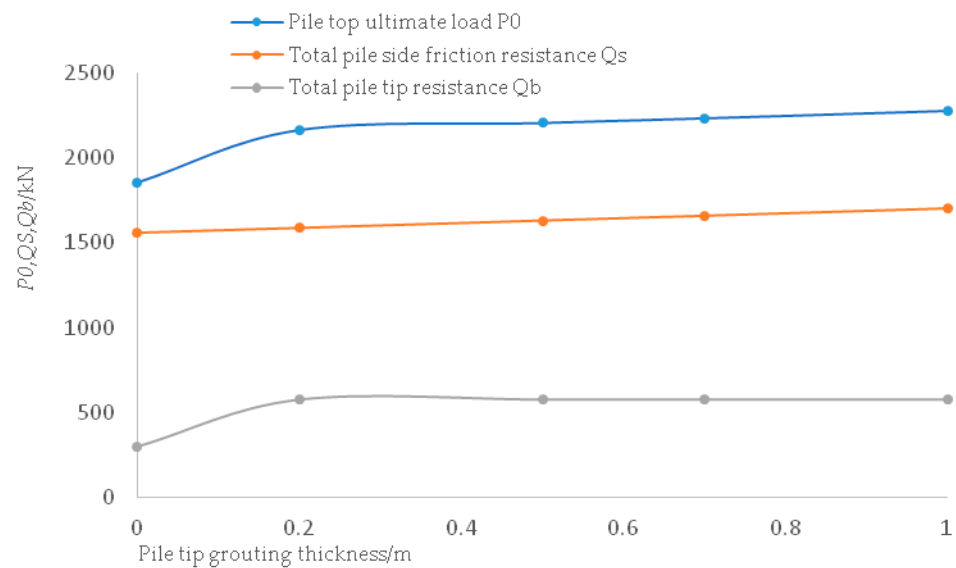


Figure 6. Relationship between P_0 , Q_s , Q_b and grouting thickness.

In order to prevent the cement soil consolidation body at the tip of the pile from punch failure [16] and considering the feasibility of practical construction, this paper suggests that the thickness of the pile tip grouting be taken as 0.5 m. Under this condition, the ultimate bearing capacity of the pile after grouting was increased from 1854 kN to 2207 kN, an increase of 19%, the total pile tip resistance was 295 kN and 577 kN before and after grouting, respectively, an increase of 96%, and the total pile side frictional resistance was 1560 kN and 1630 kN before and after grouting, respectively, an increase of only 4%. It is shown that the main thing that pile tip grouting improves is the pile tip resistance. If this grouting thickness is used for pile tip grouting, the total number of piles required can be reduced from 192 to 162 with the same total bearing capacity.

As can be seen from Figure 5, the settlement at the top of the pile corresponding to the ultimate load of the pile is 15.3 mm when the pile is ungrouted, and the settlement corresponding to the ultimate load of the pile increases as the grouting thickness increases. Settlement increased to 17.3 mm at a grouting thickness of 0.5 m, mainly due to increased settlement at the top of the pile caused by the compression of the grouting segment. If we consider that the settlement at the top of the pile is still controlled at 15.3 mm, the vertical bearing capacity of the pile with a slurry thickness of 0.5 m at the tip of the pile is 2127 kN, an increase of 14%. The total number of piles required can be reduced from 192 to 169 while ensuring the total bearing capacity remains unchanged.

4.3. Calculation of Vertical Ultimate Load under Pile Side Grouting Conditions

To analyze the effect of different grouting length ratio on the pile side on the performance of the pile, the grouting length was increased sequentially from bottom to top according to the pile segmentation, defining the grouting length ratio n as follows

$$n = \frac{L_0}{L} \quad (17)$$

where L_0 is the length of the grouting segment and L is the pile length.

The pile segmentation is calculated as before, and the parameters for the load transfer between the composite pile and the soil after grouting are still taken according to Tables 1 and 2. The calculations were carried out according to the iterative method described in Section 1, and based on the results the load settlement relationships for the pile with different grouting length ratio are shown in Figure 7.

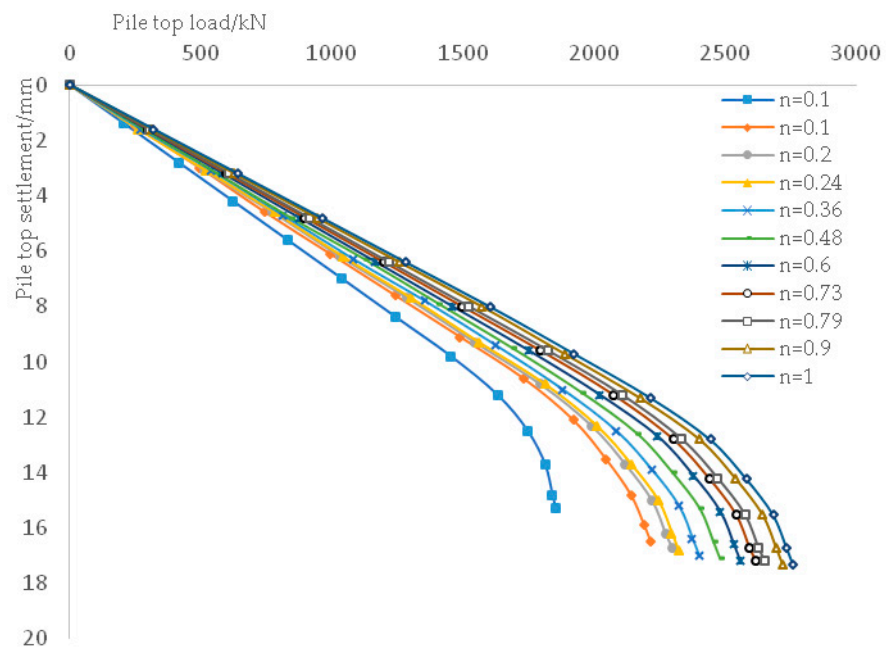


Figure 7. Load settlement relationship of pile under different grouting length ratio.

As can be seen in Figure 7, the ultimate load of the bored pile is increased after the pile side grouting and increases with the increase of the grouting length ratio. Increase in the pile axial force resulted in an increase in the pile compression and therefore in increased settlement of the pile top corresponding to the ultimate pile load capacity, which increased to 17.2 mm after full-length grouting.

To calculate the ultimate pile top load and the corresponding total pile side frictional resistance and total pile tip resistance for different grouting length ratio, the relationship between the three and the pile side grouting length ratio is shown in Figure 8.

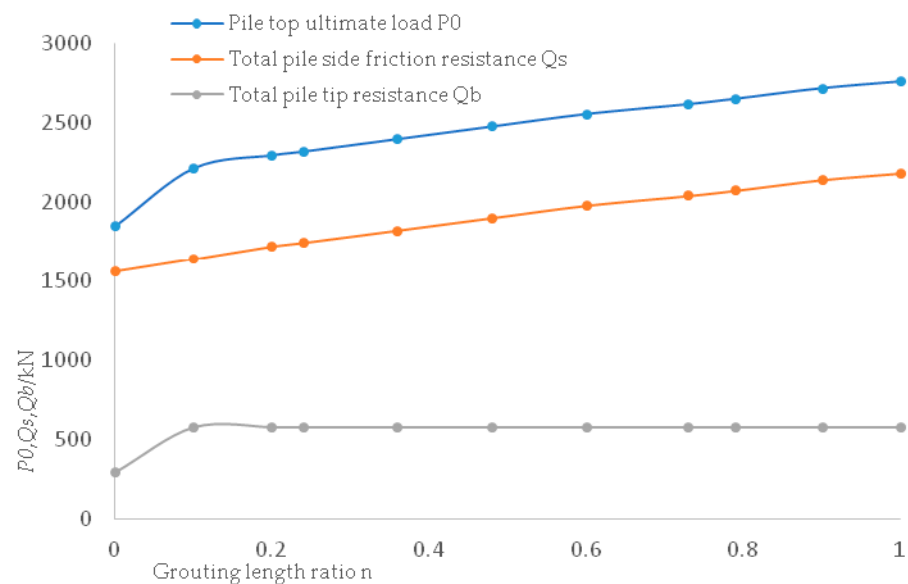


Figure 8. Relationship between P_0 , Q_s , Q_b and grouting length ratio.

From Figure 8, it can be seen that the ultimate bearing capacity of the pile is significantly increased after grouting. With the increase in the grouting length ratio, the ultimate bearing capacity of the pile also increases, and the increase of the ultimate bearing capacity of the pile is related to the increase of both the pile tip resistance and the pile side frictional

resistance. This is because the pile side grouting is done from the bottom up, so that the pile side area is slightly increased and the pile bottom cross-sectional area is increased after grouting. This results in a significant increase in pile tip resistance and only a slight increase in pile side frictional resistance. As the grouting length ratio increases the cross-sectional area at the bottom of the pile stops increasing and the total area on the side of the pile continues to increase, so the resistance at the tip of the pile stops increasing and the frictional resistance on the side of the pile continues to increase.

The ultimate pile load was increased from 1854 kN to 2761 kN after full-length pile side grouting, an increase of 49%. The total pile side frictional resistance was 1560 kN and 2184 kN before and after grouting, an increase of 40%, and the total pile tip resistance was 295 kN and 577 kN before and after grouting, an increase of 96%, indicating that pile side grouting has increased both pile side frictional resistance and pile tip resistance. If full-length pile side grouting is used, the total number of piles required can be reduced from 192 to 129, while ensuring that the total bearing capacity remains unchanged.

According to the analysis in Figure 7, if we consider that the settlement at the top of the pile is still controlled at 15.3 mm of the ungrouted pile, the bearing capacity of the pile after grouting the full length of the pile side is 2674 kN, which is an increase of 44%. The total number of piles required can be reduced from 192 to 134, while ensuring that the total bearing capacity remains unchanged.

4.4. Calculation of Vertical Ultimate Load under Composite Grouting Conditions

On the basis of studying the effect of pile tip grouting and pile side grouting on the performance of bored piles, respectively, the effect of composite grouting at the pile tip and pile side on the performance of bored piles is analyzed and the load-bearing performance of piles is calculated for a grouting thickness of 0.5 m at the pile tip and a composite grouting at the full length of the pile side. The pile segmentation for calculation as before and the load-transfer parameters between the composite pile and the soil after grouting were still taken according to Tables 1 and 2. Calculations are carried out according to the iterative method described in Section 1, and the load settlement relationship of the pile after composite grouting is derived from the calculation results, as shown in Figure 9.

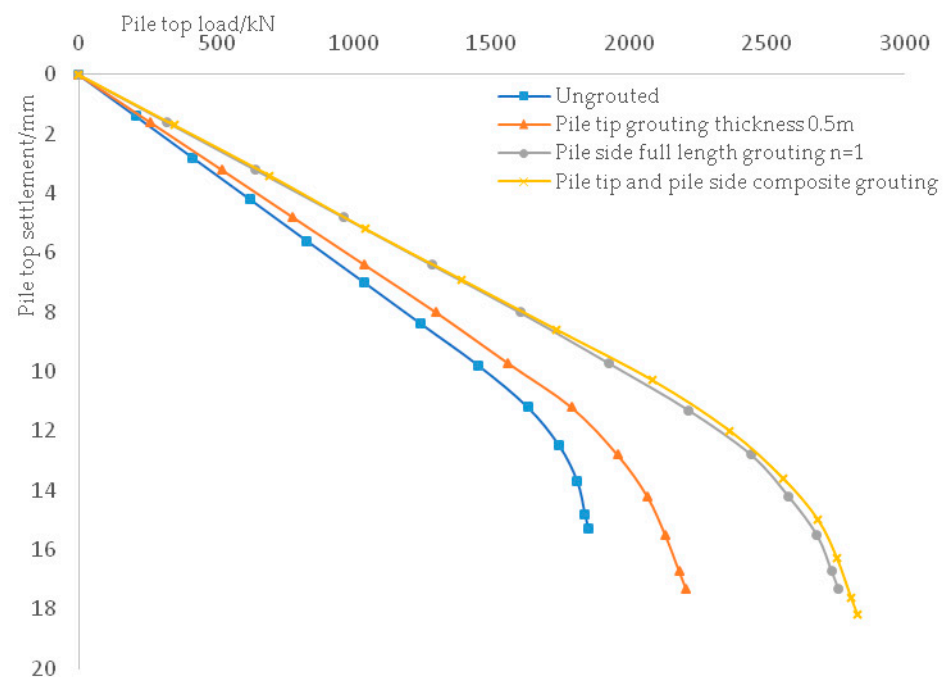


Figure 9. Load settlement relationship of piles after composite grouting.

From Figure 9, it can be concluded that the ultimate load of the pile after composite grouting is 2831 kN, which is 53% higher than that of the ungrouted pile, at which point the pile top settlement is 18.6 mm. The calculation gives the total pile side frictional resistance corresponding to the ultimate load as 2254 kN, an increase of 44% over ungrouted pile. The corresponding total pile tip resistance is 577 kN, an increase of 96% over ungrouted pile, the total number of piles required can be reduced from 192 to 126 under the condition that the total bearing capacity remains unchanged. If the settlement at the top of the pile is controlled at 15.3 mm of the ungrouted pile, the load capacity of the pile after composite grouting is 2707 kN, an increase of 46%. The total number of piles required can be reduced from 192 to 132 under the condition that the total bearing capacity remains unchanged.

5. Conclusions

In this paper, suitable diffusion radius and strength of cement soil consolidation body are selected according to the feasibility of the project. The grouting segment is considered as a composite pile and the ultimate bearing capacity of post-grouting bored piles is analyzed using the load-transfer method. The main conclusions are as follows.

(1) Pile tip grouting mainly affects the pile tip resistance and has less effect on the pile side frictional resistance.

(2) Pile side grouting has an effect on both pile side friction resistance and pile tip resistance, and pile side frictional resistance increases with increase of grouting length ratio.

(3) The ultimate bearing capacity of the pile was increased by the pile tip grouting, the pile side full-length grouting, and the composite grouting. The ultimate bearing capacity was increased by 19%, 49%, and 53% respectively, compared to that before grouting.

(4) After reaching the ultimate bearing capacity, the settlement of the pile tops of the grouting piles all increased. If the settlement of the pile tops is guaranteed to be the same as that of the ungrouted piles. The bearing capacity of the piles can also be increased by 14%, 44%, and 46%, respectively, after pile tip grouting, pile side full-length grouting, and composite grouting according to settlement control.

(5) The increase in the bearing capacity of the pile after grouting can reduce the number of piles used in the project while ensuring the total bearing capacity remains unchanged.

Author Contributions: Data curation, H.L.; Investigation, W.G.; Supervision, D.K.; Writing—original draft, H.L.; Writing—review & editing, D.K. All authors have read and agreed to the published version of the manuscript.

Funding: This research received no external funding.

Conflicts of Interest: The authors declare no conflict of interest.

References

1. Li, Y.H.; Zhu, X.; Zhou, T.H. Experimental study of effects of pile tip post grouting on bearing characteristics of large-diameter bored pile. *Geotech. Mech.* **2016**, *37*, 388–396. (In Chinese)
2. Huang, S.G.; Shen, J.H.; Li, M. Reliability analysis of bearing capacity of post-grouted bored piles. *Rock Soil Mech.* **2019**, *40*, 1977–1982. (In Chinese)
3. Bruce, D.A. Enhancing the performance of large diameter piles by grouting. *Ground Eng.* **1986**, *19*, 9–15.
4. Bu, K.M.; Yin, K.L.; Gong, W.M. Post-grouting technique for piled foundation: Case history of Su-Tong Bridge. *Rock Soil Mech.* **2008**, *29*, 1697–1700. (In Chinese)
5. Zhai, D.Z.; Zhou, F.; Zhou, J.F.; Zhu, R. *Experimental Study and Numerical Analysis on Bearing Characteristics of Large Diameter Ultra-Long Bored Piles with Post Grouting on the Tip and Side*; IOP Conference Series; Earth and Environmental Science: Qingdao, China, 2018; p. 022024.
6. Wan, Z.H.; Dai, G.L.; Gao, L.C.; Gong, W.M. Study on practical calculation method of bearing capacity and settlement of large diameter post-grouting bored pile. *Rock Soil Mech.* **2020**, *41*, 2746–2755. (In Chinese)
7. Fang, K.; Zhang, Z.M.; Liu, Z.J.; Liu, X.W. Load settlement relationship prediction for grouted pile based on load transfer function method. *J. Harbin Inst. Technol.* **2012**, *44*, 95–99. (In Chinese)
8. Seed, H.B.; Reese, L.C. The action of soft clay along frictional piles. *Trans. ASCE* **1957**, *122*, 731–754.
9. Kezdi, S. Bearing mechanism of piles. *Géotechnique* **1965**, *20*, 1–5.

10. Fang, W.M.; Zhao, M.H.; Su, Z. Analysis of vertical ultimate bearing capacity of piles controlled by settlement. *Cent. South Highw. Eng.* **1999**, *24*, 25–27. (In Chinese)
11. Kraft, L.M.; Ray, R.P.; Kagawa, T. Theoretical t-z curves. *Geotech. Eng. Div.* **1981**, *107*, 1543–1561. [[CrossRef](#)]
12. Kezdi, A. The bearing capacity of pile and pile groups. In Proceedings of the 4th International Conference on Soil Mechanics and Foundation Engineering, London, UK, 12–24 August 1957; Volume 2, pp. 46–51.
13. Brown, D.R.; Warner, J. Compaction Grouting. *Soil Mech. Found. Div. J. ASCE* **1973**, *99*, 589–601. [[CrossRef](#)]
14. Zou, J.F.; Li, L.; Yang, X.L.; Hu, Z.N. Mechanism analysis of fracture grouting in soil. *Rock Soil Mech.* **2006**, *27*, 625–628 + 642. (In Chinese)
15. Kuang, J.Z. *Geotechnical Grouting Theory and Engineering Examples*; Science Press: Beijing, China, 2001. (In Chinese)
16. ACI Committee 326. Shear and Diagonal Tension. *ACI J. Proc.* **1962**, *59*, 1–30.